

LETTER TO THE EDITOR

Discovery of an old photoevaporating disk in σ Orionis[★]

E. Rigliaco^{1,2}, A. Natta¹, S. Randich^{1,2}, and G. Sacco³

¹ Osservatorio Astrofisico di Arcetri, INAF, Largo E. Fermi 5, 50125 Firenze, Italy
e-mail: erigliaco@arcetri.astro.it

² Università di Firenze, Dipartimento di Astronomia, Largo E. Fermi 2, 50125 Firenze, Italy

³ Osservatorio Astronomico di Palermo, INAF, Piazza del Parlamento 1, 90134 Palermo, Italy

Received 17 December 2008 / Accepted 2 February 2009

ABSTRACT

The photoevaporation of circumstellar disks is a powerful process in the disk dissipation at the origin of the Orion proplyds. This Letter reports the first detection of a photoevaporating disk in the final but long-lasting phase of its evolution. The disk is associated to a low-mass T Tauri member of the σ Ori Cluster. It is characterized by a very low (if any) accretion rate and by a tenuous ($\dot{M}_{\text{loss}} \sim 10^{-9} M_{\odot}/\text{yr}$) photoevaporation wind, which is unambiguously detected in the optical spectrum of the object. The wind emits strong forbidden lines of [SII] and [NII] because the low-mass star is close to a powerful source of ionizing photons, the O9.5 star σ Ori.

Key words. stars: formation – accretion, accretion disks

1. Introduction

The evolution of circumstellar disks surrounding low-mass T Tauri stars (TTS in the following) is controlled by the interplay of different physical processes, which include viscous accretion onto the central star, photoevaporation by the stellar radiation field, and planet formation. If the low-mass star is sufficiently close to a more massive and hotter object, photoevaporation by this external source of high-energy radiation is also important because it can dominate the disk evolution.

The process of photoevaporation has been extensively discussed (see, e.g. Hollenbach et al. PPIV; Dullemond et al. PPV). High-energy photons heat gas disks to temperatures such that the thermal pressure exceeds the gravity from the central star. The disk evaporates from outside-in, with a mass-loss rate that decreases with time as the disk shrinks. Most of the well-studied Orion proplyds are caught in the first, short evolutionary phase, when the mass-loss rate is very high ($\dot{M}_{\text{loss}} > 10^{-7} M_{\odot}/\text{yr}$, Henney et al. 1999).

We report in this Letter on the first detection of a proplyd in a much later evolutionary phase, when the mass-loss rate is $\ll 10^{-8} M_{\odot}/\text{yr}$. The object (a low-mass TTS) is located in the star-forming region σ Ori (age $\sim 2\text{--}3$ Myr), which contains the massive quintuplet system σ Ori. The brightest star of this system (spectral type O9.5) forms a large, low-density HII region (Habart et al. 2005) and the bright PDR known as the Horsehead (Abergel et al. 2003). The low background from the HII region and the relatively short distance (~ 400 pc; Mayne & Naylor 2008) allow us to detect the slow photoevaporated TTS wind and to measure its optical line emission spectrum.

2. The T Tauri star SO587

2.1. Stellar properties

SO587 (also identified as R053833-0236 Wolk 1996 or Mayrit 165257 Caballero 2008) ($\alpha_{2000} = +05:38:34.04$, $\delta_{2000} = -02:36:37.33$) has been classified as M3–M4 by Zapatero-Osorio et al. (2002) on the basis of low-resolution optical spectra ($T_{\text{eff}} \sim 3300$ K). The optical extinction is negligible (Oliveira et al. 2004), and we estimate a luminosity of $0.3 \pm 0.1 L_{\odot}$, based on this spectral type and the V , R , I magnitudes (Wolk 1996). The corresponding mass is about $0.2 M_{\odot}$, both from D’Antona & Mazzitelli (1997) and Baraffe et al. (1998) evolutionary tracks. Based on its location on the HR diagram, SO587 has an age of ~ 1 Myr, apparently slightly younger than the bulk of the σ Ori stars. SO587 is an X-ray source, with luminosity $L_X \sim 10^{29}$ erg/s (Franciosi et al. 2006).

2.2. Disk properties

SO587 is detected by Spitzer at all IRAC wavelengths and at $24 \mu\text{m}$ with MIPS. It shows a relatively weak excess emission, and is classified as an evolved disk (EV, Hernandez et al. 2007). We confirm this classification. The IR emission is reproduced well by a geometrically flat, optically thick disk heated by the central star, seen at an inclination of about 40 deg. The outer disk radius is not constrained by the existing infrared photometry, which is limited to $24 \mu\text{m}$, as long as $R_{\text{out}} \gtrsim 1\text{--}2$ AU. The model is not unique but exploration of a large number of disk models rules out optically thin disks, which have different Spitzer colors and lower luminosity than observed in SO587 ($L_{\text{disk}}/L_{\text{star}} \sim 0.07$) (see Cieza et al. 2007). Also, there is no evidence in the SED of the large inner holes (few AU) seen in transitional disks (Chiang & Murray-Clay 2007, and references therein), as all the models that fit the data have inner radii $\lesssim 0.1$ AU.

[★] Based on observations collected at the European Southern Observatory, Chile. Program 074.D-0136(A).

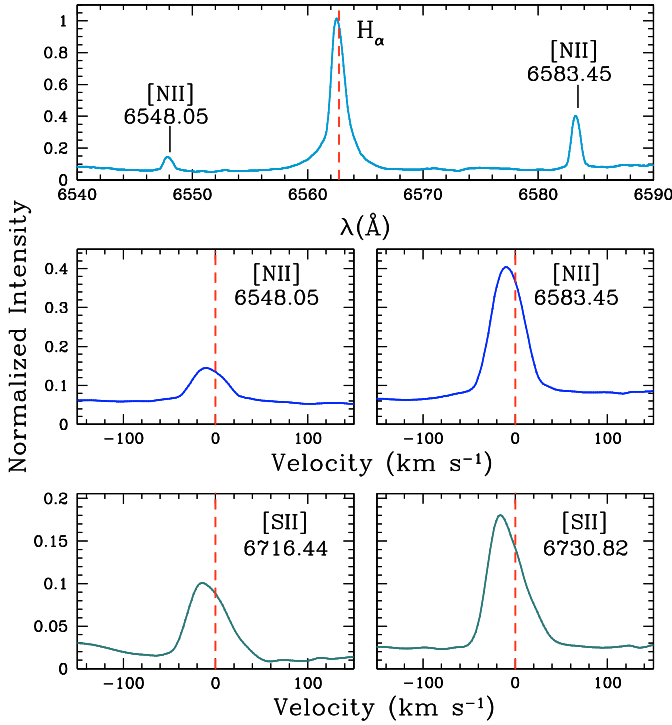


Fig. 1. The top panel shows the spectrum in the $H\alpha$ region, with $H\alpha$ and the two $[\text{NII}]\lambda 6548.05$ and $[\text{NII}]\lambda 6583.45$ lines. Middle panel: $[\text{NII}]\lambda 6548.05$ and $[\text{NII}]\lambda 6583.45$ line profiles as function of the velocity shift with respect to the stellar velocity (vertical dashed line). Bottom panel: same for $[\text{SII}]\lambda 6716.64$ and $[\text{SII}]\lambda 6730.82$, as label.

2.3. Accretion rate

SO587 shows no evidence of significant accretion onto the central star. An estimate of \dot{M}_{acc} can be obtained from the U band magnitude 18.5 ± 0.8 measured by Wolk (1996). For the spectral type and luminosity of SO587, this corresponds to an excess U band emission of 1 mag at most. Using the correlation between the U band excess emission and the accretion luminosity established by Gullbring et al. (1998) for TTS, we derive $L_{\text{acc}} \sim 3 \times 10^{-3} L_{\odot}$ with an uncertainty of a factor 2, i.e., about 1% of the stellar luminosity. Since a comparable U band excess emission may be due to chromospheric activity (White & Ghez 2001), this is likely an upper limit to L_{acc} . The corresponding accretion rate is $\lesssim 3 \times 10^{-10} M_{\odot}/\text{yr}$.

3. The optical spectrum

SO587 was observed by Sacco et al. (2008) using the multi-object instrument FLAMES on VLT/UT2 and Giraffe spectrograph with the HR15N grating (6470–6790 Å, spectral resolution $R = 17000$). The observations were obtained in 6 separate runs of 1 h each in October and December 2004. Details on the observations and data reduction, in particular on sky subtraction, can be found in Sacco et al. (2008). The spectra of SO587 show $H\alpha$ in emission, as well as strong forbidden lines from $[\text{NII}]$ at 6548 and 6583 Å and $[\text{SII}]$ at 6716 and 6731 Å (Fig. 1). Table 1 gives the pseudo-equivalent width (pEW) of each line (negative values for emission lines), the $FWHM$ (not corrected for the instrumental resolution of about 20 km s^{-1}), and the line luminosities. The contribution to the lines (both $H\alpha$ and the

Table 1. Characteristics of the emission lines.

Line	λ (Å)	pEW (Å)	$FWHM$ (km s^{-1})	Luminosity $10^{-5} L_{\odot}$
$H\alpha$	6562.71	-15.2 ± 0.1	69.9 ± 2	12.0 ± 0.1
$[\text{NII}]$	6548.05	-0.82 ± 0.2	42.6 ± 1	0.6 ± 0.15
$[\text{NII}]$	6583.45	-2.46 ± 0.1	39.6 ± 0.5	1.9 ± 0.1
$[\text{SII}]$	6716.44	-1.22 ± 0.03	48.7 ± 0.4	0.6 ± 0.02
$[\text{SII}]$	6730.82	-1.60 ± 0.08	43.2 ± 0.4	0.8 ± 0.04

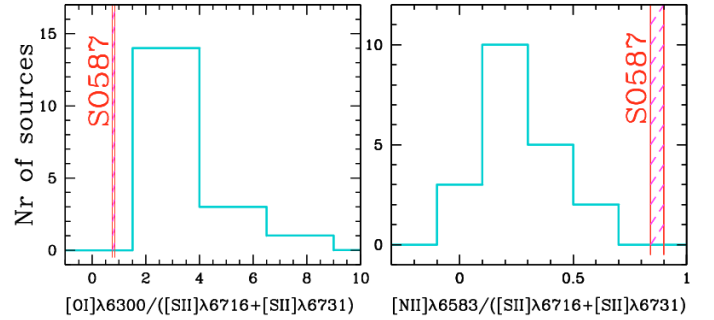


Fig. 2. Distribution of the ratios $[\text{OI}]\lambda 6300 / ([\text{SII}]\lambda 6716 + [\text{SII}]\lambda 6731)$ and $[\text{NII}]\lambda 6583 / ([\text{SII}]\lambda 6716 + [\text{SII}]\lambda 6731)$ among the Hartigan et al. (1995) Taurus TTS with detected lines. The magenta dashed region shows the location of SO587 considering the errors on the line equivalent widths; $[\text{OI}]\lambda 6300$ from Zapatero-Osorio et al. (2002).

forbidden lines) of the extended HII region due to the O9.5 star σ Ori is negligible.

The line luminosities were computed using the observed R magnitude to calibrate the continuum flux and the wavelength dependence within the band appropriate for a 3300 K star. The luminosity is of the order of $10^{-5} L_{\odot}$ for all the forbidden lines.

Zapatero-Osorio et al. (2002) also detected $H\alpha$ and forbidden emission lines in two of their low-resolution spectra with highest quality, but not in the other, lower-quality spectra; when detected, the pEW of the lines are similar to our values. We checked for evidence of line variability in the Sacco et al. spectra, and found none. The line profiles and intensities are very similar in each run, with the pEW varying $\sim 10\%$.

In the two spectra where emission lines were detected, Zapatero-Osorio et al. (2002) also measured the pEW of the two oxygen lines at 6300 and 6364 Å, which are outside our spectral range. The corresponding luminosity is $1.2 \pm 0.06 \times 10^{-5} L_{\odot}$ for the 6300 Å line and $0.4 \pm 0.03 \times 10^{-5} L_{\odot}$ for the 6364 Å one, similar to the $[\text{SII}]$ and $[\text{NII}]$ line luminosity.

4. Not an accretion-driven wind

The forbidden lines detected in SO587 are seen in many TTS, and are usually interpreted in the framework of accretion-driven winds (e.g. Ferreira et al. 2006, and reference therein). These centrifugally-driven MHD winds originate in the inner disk and move fast. An estimate of the average mass-loss rate can be obtained from the luminosity of the forbidden lines, following Hartigan et al. (1995). Taking, e.g., the $[\text{SII}]\lambda 6731$ line, this is

$$\dot{M}_{\text{wind}} = 3.38 \times 10^{-8} \left(1 + \frac{n_c}{n_e} \right) \left(\frac{L_{6731}}{10^{-4} L_{\odot}} \right) \times \left(\frac{V_{\perp}}{150 \text{ km s}^{-1}} \right) \left(\frac{l_{\perp}}{2 \times 10^{15} \text{ cm}} \right)^{-1} M_{\odot}/\text{yr}. \quad (1)$$

The electron density n_e , derived from the ratio of the two [SII] lines, is $\sim 1.5 \times 10^3 \text{ cm}^{-3}$, well below the critical density n_c , which is $\sim 1.3 \times 10^4 \text{ cm}^{-3}$. Assuming that all S is SII, a S abundance of 1.6×10^{-5} , a typical value of $V_\perp \sim 150 \text{ km s}^{-1}$ for the outflow velocity and that the outflow fills our beam of 1 arc-sec ($l_\perp \sim 6 \times 10^{15} \text{ cm}$), we derive a mass-loss rate of about $10^{-8} M_\odot/\text{yr}$.

This value of \dot{M}_{wind} is high for a $0.2 M_\odot$ TTS (Hartigan et al. 1995). It is particularly high when compared to \dot{M}_{acc} , as $\dot{M}_{\text{wind}}/\dot{M}_{\text{acc}} \geq 10$. In TTS, this ratio is <1 and <0.1 in the majority of cases (Hartigan et al. 1995; White & Hillenbrand 2004), in agreement with the expectations of accretion-driven jets and winds (e.g., Shu et al. 1994; Pudritz et al. 2007). Even taking the uncertainties on the assumptions entering into Eq. (1) into account (see Cabrit 2002), the very high value of the ratio $\dot{M}_{\text{wind}}/\dot{M}_{\text{acc}}$ makes it unlikely that the forbidden lines in SO587 could be emitted by an accretion-driven wind.

5. Line profiles

Additional evidence that the SO587 forbidden lines do not originate in an accretion-driven wind is provided by a comparison of the forbidden line luminosities and profiles with those of classical TTS. We first notice the strength of the [NII] lines, which are weak or absent in TTS, but comparable in luminosity to the [SII] lines in SO587. Strong [NII] lines are expected in highly ionized gas, as in HII regions or in the bow shocks at the head of jets, and are weaker than the other forbidden lines in the partially neutral wind/jets of TTS. SO587 is also unusual in having strong [SII] lines with respect to the [OI] lines (Fig. 2).

Moreover, the profiles of the SO587 [SII] and [NII] lines differ from the typical TTS line profiles. The [SII] and [NII] are resolved in our spectra, and they show a small shift of the peak to the blue ($\lesssim 10\text{--}14 \text{ km s}^{-1}$), a steep rise in the blue, and a slow decline in the red wing. Spatially unresolved profiles of the [SII] 6731 Å line in a sample of accreting TTS typically show larger peak blueshifts ($\sim 80\text{--}100 \text{ km s}^{-1}$), and significantly more emission in the blue than in the red wing (Edwards et al. 1987; Hartigan et al. 1995). In fact, these asymmetries are interpreted as evidence that the disk obscures the receding portion of the line emitting region.

The high luminosity in [NII], the low ratio [OI]/[SII] ~ 1 , and the details of the line profiles of SO587 are strongly reminiscent of the properties of the Orion proplyds (Bally et al. 1998; Henney & O'Dell 1999). The Orion proplyds are interpreted as the result of photoevaporation of the disk by the hot Trapezium stars (see, e.g. Hollenbach et al. PPIV). The optical forbidden lines of ionized species, such as [SII] and [NII], are formed in the outer part of the outflow, which is ionized, heated, and shocked by the radiation and wind of $\theta^1 C$ Ori (Garcia-Arredondo et al. 2001).

6. A photoevaporating disk

We propose that SO587 is a photoevaporating disk, which we detect in optical forbidden lines because it is ionized by the nearby (projected distance of $\sim 0.35 \text{ pc}$) O9.5 star σ Ori. Let us assume that the SO587 disk loses mass at a rate \dot{M}_{loss} . Whatever the source of the photoevaporating photons (the central star or σ Ori – see below), this wind originates in the outer disk, and is slow (few km s^{-1}) and neutral. However, the high-energy

($h\nu > 13.6 \text{ eV}$) photons from σ Ori ionize the outflowing gas to a distance r_{IF} from SO587 roughly

$$r_{\text{IF}} \sim 1.6 \times \left(\frac{\dot{M}_{\text{loss}}}{\mu_{\text{H}} v_{\text{IF}}} \right)^{2/3} \left(\frac{\alpha \Delta^2}{\Phi_i} \right)^{1/3}. \quad (2)$$

Here α is the recombination coefficient ($\alpha = 2.6 \times 10^{-13} \text{ cm}^3 \text{ s}^{-1}$), μ_{H} the mean molecular weight Φ_i the high energy flux from σ Ori ($\Phi_i \sim 10^{48}$ photons/s; Peimbert & Rayo 1975), Δ is the distance between SO587 and σ Ori, and $v_{\text{IF}} \sim 10 \text{ km s}^{-1}$ the velocity at the ionization front (Stöerzer & Hollenbach 1999), so that

$$r_{\text{IF}} \sim 80 \text{ AU} \left(\frac{\dot{M}_{\text{loss}}}{10^{-9} M_\odot/\text{yr}} \right)^{2/3} \left(\frac{\Delta}{0.35 \text{ pc}} \right)^{2/3}. \quad (3)$$

The ionization front moves away from SO587 and is closer to σ Ori, if either \dot{M}_{loss} and/or the distance between the two stars increases. The optical forbidden lines shown in Fig. 1 can only come from the ionized regions of the outflow; since they are detected in spectra taken with a beam of radius $\sim 200 \text{ AU}$ centered on SO587, it must be $r_{\text{IF}} \ll 200 \text{ AU}$. This condition is verified for $\dot{M}_{\text{loss}} \lesssim 10^{-9} M_\odot/\text{yr}$; if \dot{M}_{loss} is significantly higher, r_{IF} moves too far from SO587, and the outflow region within the beam is all neutral.

In this model, the [SII] and [NII] forbidden lines originate mostly in the ionized gas at r_{IF} . For $\dot{M}_{\text{loss}} = 10^{-9} M_\odot/\text{yr}$, the electron density at r_{IF} from the continuity equation ($n_e = \dot{M}_{\text{loss}}/(4\pi r_{\text{IF}}^2 \mu_{\text{H}} v_{\text{IF}})$) is $\sim 2 \times 10^3 \text{ cm}^{-3}$, in good agreement with the electron density derived from the observed ratio of the two [SII] lines ($\sim 1.5 \times 10^3 \text{ cm}^{-3}$; Sect. 4). The [SII] 6731 Å line luminosity within the beam, computed assuming that all S in SII and a temperature $\sim 10^4 \text{ K}$, is $\sim 10^{-5} L_\odot$, in good agreement with the observations.

What is the origin of this outflow? Both the SO587 star and σ Ori can, in principle, cause disk photoevaporation, and the properties of the outflow are, qualitatively, similar. Let us consider first the case of disk photoevaporation due to the FUV ($6 \text{ eV} < h\nu < 13.6 \text{ eV}$) radiation of σ Ori. Adams et al. (2004) have computed detailed models of the photoevaporation by an external source of disks around stars of different masses. At a distance of 0.35 pc , the FUV radiation field from σ Ori is $G_0 \sim 10^4$ (in units of the Habing radiation field; Abergel et al. 2003). Let us assume that the SO587 disk has mass $\sim 0.05 M_{\text{star}}$ when the outer radius is $\sim 60 \text{ AU}$ and surface density $\propto R^{-1}$. If we take Adams et al. (2004) results for a star of central mass $0.25 M_\odot$ in a radiation field $G_0 = 3000$ (the exact value of G_0 is not crucial as long as it is higher than this value), the disk has a first, evolutionary stage characterized by a relatively large size and high mass-loss rates $\sim \text{few} \times 10^{-8} M_\odot/\text{yr}$. This phase is rapid, and the disk loses about 80% of its mass in $\sim 3 \times 10^5 \text{ yr}$. By that time, the disk radius is $R_d \sim 10 \text{ AU}$, and the mass loss rate is $\sim 10^{-9} M_\odot/\text{yr}$. In this later evolutionary stage, the small, slowly evaporating disk has a lifetime of $\sim 2 \times 10^6 \text{ yr}$, comparable to the age of SO587 itself.

This scenario can explain our data, as long as SO587 stays in the vicinity of σ Ori for $\geq 10^6 \text{ yr}$. With a velocity dispersion of $\sigma \sim 1 \text{ km s}^{-1}$ in the radial direction (Sacco et al. 2008), the distance between σ Ori and SO587 can increase to $\sim 1 \text{ pc}$ in 10^6 yr , i.e., about 3 times the present projected distance. This is still consistent with the constraints we have set at the beginning of this section, although marginally so.

However, it is possible that the photoevaporation of the SO587 disk is caused by the high-energy radiation from the central star. Recently, Gorti & Hollenbach (2008) model the case of

a low mass TTS ($0.3 M_{\odot}$), with properties roughly comparable to those of SO587. The trend of \dot{M}_{loss} with time is similar, with an early phase when the disk is large and $\dot{M}_{\text{loss}} \gtrsim 10^{-8} M_{\odot}/\text{yr}$, followed by a decrease in the disk radius and of \dot{M}_{loss} . The phase with $\dot{M}_{\text{loss}} \sim 10^{-9} M_{\odot}/\text{yr}$, $R_d \sim 30$ AU has a lifetime of about 5×10^6 yr, which can account for the SO587 observed properties.

In both cases, a first period of rapid evaporation, which produces a significant reduction of the disk size, is followed by a phase of slower evolution, with correspondingly lower values of \dot{M}_{loss} . We think that SO587 is in this late evolutionary stage, because its disk has shrunk to 10–30 AU in radius and is now in the last, long phase of slow photoevaporation. SO587 shines in the optical forbidden lines of species, such as [SII] and [NII], only because it is at the right distance from σ Ori at the time of our observations.

The exact values of \dot{M}_{loss} , the location of the ionization front, the dynamics of the gas, and in particular the line profiles are all the result of the interaction of several complex physical processes, that need to be explored. We note, for example, that the observed profiles of the optical forbidden lines require a line-emitting region to be much larger than the disk, which does not seem to obscure the receding part of the outflow. Observationally, there are several possible tests. The disk size can be constrained directly by spatially resolved observations at millimeter wavelengths, but also indirectly by photometry at far-infrared wavelengths. Also, a basic feature of externally photoevaporated disks is the displacement between the ionization front and the star; in SO587 this is predicted to be ~ 0.25 arcsec, detectable with spectroastrometric techniques or by direct imaging from HST.

7. Discussion and conclusions

The possibility that we are detecting the final, but long-lasting stages of the dissipation of a disk by photoevaporation is intriguing.

As mentioned in Sect. 1, σ Ori is particularly suited to this kind of study. First of all, the low background emission is very favorable for detecting objects, such as SO587, with a mass-loss rate at least two orders of magnitude lower than that of the Orion proplyds, and, more generally, for studying the effects of an external, high-energy radiation field on jets (Andrews et al. 2004) and disks.

A second important point is the age of σ Ori (2–3 Myr), significantly more than of Orion, such that disks have had enough time to evolve to the stage of low-accretion rate, low photoevaporation mass loss. We note that $\dot{M}_{\text{loss}} \sim \dot{M}_{\text{acc}} \sim 10^{-9} M_{\odot}/\text{yr}$ in SO587, as expected at time $\gtrsim 10^6$ yr in disk evolution models where the photoevaporation by an external source is coupled to viscous evolution (Clarke 2007).

Some disks, such as SO587, show evidence of grain growth and settling in their SEDs, and it seems possible not only to detect old photoevaporated disks but also to relate their

properties to those of the grains. Larger grains have two competing effects on the photoevaporation process: on the one hand, they have lower extinction in the FUV, allowing the FUV radiation to penetrate more deeply into the disk; on the other, the heating efficiency will be lower. The balance between these two competing effects needs to be explored in the model calculations, but can also be addressed observationally.

Within 0.4 pc around σ Ori Hernandez et al. (2007) detect about 30 objects with all kinds of disks (Class II, Class III, and EV). The spread of SEDs probably reflects a varying degree of dust evolution (Dullemond & Dominik 2004; D’Alessio et al. 2006). We are currently carrying on a comprehensive study of the accretion and mass-loss properties of σ Ori objects to identify other proplyds and to address some of the issues mentioned in this section.

Acknowledgements. We would like to thank S. Wolk and D. Hollenbach for useful discussions. We also thank the anonymous referee for comments that clarified the paper.

References

- Abergel, A., Teysier, D., Bernard, J. P., et al. 2003, A&A, 410, 577
 Adams, F. C., Hollenbach, D., Laughlin, G., et al. 2004, ApJ, 611, 360
 Andrews, S. M., Reipurth, B., Bally, J., et al. 2004, ApJ, 606, 353
 Bally, J., Sutherland, R. S., Devine, D., et al. 1998, AJ, 116, 854
 Baraffe, I., Chabrier, G., Allard, F., et al. 1998, A&A, 337, 403
 Caballero, J. A. 2008, A&A, 478, 667
 Cabrit, S. 2002, EAS Publ. Ser., 3, 147
 Chiang, E., & Murray-Clay, R. 2007, NatPh, 3, 604
 Cieza, L. A., Padgett, D., Stapelfeldt, K. R., et al. 2007, ApJ, 667, 308
 Clarke, C. J. 2007, MNRAS, 376, 1350
 D’Alessio, P., Calvet, N., Hartmann, L., et al. 2006, ApJ, 638, 314
 D’Antona, F., & Mazzitelli, I. 1997, Mem. Soc. Astr. It., 68, 807
 Dullemond, C. P., & Dominik, C. 2004, A&A, 421, 1075
 Dullemond, C. P., Hollenbach, D., Kamp, I., et al. 2007, PPV, 555
 Edwards, S., Cabrit, S., Strom, S. E., Heyer, I., & Strom, K. M. 1987, ApJ, 321, 473
 Ferreira, J., Dougados, C., & Cabrit, S. 2006, A&A, 453, 796
 Franciosini, E., Pallavicini, R., & Sanz-Forcada, J. 2006, A&A, 446, 501
 Garcia-Arredondo, F., Henney, W. J., & Arthur, S. J. 2001, ApJ, 561, 830
 Gorti, U., & Hollenbach, D. 2008 [arXiv:0809.1494]
 Gullbring, E., Hartmann, L., Briceño, C., et al. 1998, ApJ, 492, 323
 Habart, E., Abergel, A., Walmsley, C. M., et al. 2005, A&A, 437, 177
 Hartigan, P., Edwards, S., & Ghandour, L. 1995, ApJ, 452, 736
 Henney, W. J., & O’Dell, C. R. 1999, AJ, 118, 2350
 Hernandez, J., Hartmann, L., Megeath, T., et al. 2007, ApJ, 662, 1067
 Hollenbach, D. J., Yorke, H. W., & Johnstone, D. 2000, PPIV, 401
 Mayne, N. J., & Naylor, T. 2008, MNRAS, 386, 261
 Oliveira, J. M., Jeffries, R. D., & van Loon, J. T. 2004, MNRAS, 347, 1327
 Peimbert, M., & Rayo, J. F. 1975, RMxAA, 1, 289
 Pudritz, R. E., Ouyed, R., et al. 2007, PPV, 277
 Sacco, G., Franciosini, F., Randich, S., et al. 2008, A&A, 488, 167
 Shu, F. H., Nijita, J., Ostriker, E., et al. 1994, ApJ, 429, 781
 Störzer, H., & Hollenbach, D. 1998, ApJ, 515, 669
 White, R. J., & Ghez, A. M. 2001, ApJ, 556, 265
 White, R. J., & Hillenbrand, L. A. 2004, ApJ, 616, 998
 Wolk, S. J. 1996, Ph.D. Thesis, State Univ. (New York: Stony Brook)
 Zapatero-Osorio, M. R., Béjar, V. J. S., Pavlenko, Ya., et al. 2002, A&A, 384, 937